

## ARTICLE

## Metal-Triggered DNA Folding by Different Mechanisms

Wei Deng<sup>a</sup>, Bin Zheng<sup>c</sup>, Wei Ding<sup>a</sup>, Hong Zhu<sup>a</sup>, Hao-jun Liang<sup>a,b\*</sup>*a. Department of Polymer Science and Engineering, University of Science and Technology of China, Hefei 230026, China**b. CAS Key Laboratory of Soft Matter Chemistry, University of Science and Technology of China, Hefei 230026, China**c. School of Chemistry and Chemical Engineering, Hefei Normal University, Hefei 230061, China*

(Dated: Received on March 27, 2015; Accepted on May 13, 2015)

Metal-mediated base pairs by the interaction between metal ions and artificial bases in oligonucleotides has been widely used in DNA nanotechnology and biosensing technique. Using isothermal titration calorimetry, circular dichroism spectroscopy and fluorescence spectroscopy, the folding process of T-C-rich oligonucleotides (TCO) induced by  $\text{Hg}^{2+}$  and  $\text{Ag}^+$  with the synthetic sequence d(T6C6T6C6T6C6T6) was studied and analyzed. Although thermodynamic data predict that TCO should initially fold into a relatively stable hairpin through two possible pathways of conformational transitions whether  $\text{Hg}^{2+}$  or  $\text{Ag}^+$  were added at first, the mechanisms and final products between the two are entirely different from isothermal titration calorimetry outcomes. When  $\text{Hg}^{2+}$  were added first, the hairpin was formed through T-Hg-T structure with further stabilization by C-Ag-C after  $\text{Ag}^+$  addition. However, it is proposed that an unusual metal-base pair for  $\text{Ag}^+$  binding is generated instead classical C-Ag-C when  $\text{Ag}^+$  was injected first. Moreover, further confirmation of this unconventional metal-base pair T-Ag-C was verified by circular dichroism and fluorescence spectroscopy.

**Key words:** Metal-mediated base pairs,  $\text{Hg}^{2+}$  and  $\text{Ag}^+$ , T-C-rich oligonucleotides, Folding mechanisms, T-Ag-C base pair

## I. INTRODUCTION

The specific hydrogen bonding of DNA base pairs provides the chemical foundation for genetics. This powerful molecular recognition system and DNA possessing appealing features such as its minuscule size, short structural repeat and rigidity on nanoscale, can be used in nanotechnology to direct the assembly of highly structured materials with specific nanoscale features [1–4]. Their applicability can be extended even further by the introduction of functional groups such as metal ions [5, 6]. One recently established method for the site-specific functionalization of nucleic acids with metal ions is based on the use of metal-mediated base pairs. Such base pairs are formed by coordinative bonds between metal ions and nucleobases instead of normal hydrogen bonding [7–10]. Compared with other types of unnatural base pairs based upon rearrangement of the hydrogen-bonding pattern or shape complementarity, metal-mediated base pairs have the advantage of incorporation of different metal ions which can endow

unique chemical and physical properties. It has been reported that many metal ions, such as  $\text{Hg}^{2+}$ ,  $\text{Ag}^+$ ,  $\text{Cu}^{2+}$ ,  $\text{Ni}^{2+}$  and  $\text{Zn}^{2+}$ , can specifically interact with nucleoside bases to form metal-ion-mediated base pairs [11–17]. For example, it is well-known that thymine-thymine (T-T) and cytosine-cytosine (C-C) mispairs selectively captured  $\text{Hg}^{2+}$  and  $\text{Ag}^+$  respectively [12, 18, 19]. Moreover, a T-C pair could be moderately stabilized by either  $\text{Hg}^{2+}$  or  $\text{Ag}^+$  [20, 21]. Other forms of metal-base pairs were gradually discovered [21–23]. As metal-base pairs are highly selective and sensitive for specific metal ions, extremely wide range of applications such as DNA sensor for detecting metal ions [24–28] DNA detection triggered by metal ions [29], construction of DNA nanomachine and nano-device [30–33] and fabrication of molecular-scale logic gate [34–36], have been widely developed.

Recently, research interests gradually turned to foundational theories research [37, 38]. Wells and Hiraio carried out theoretical calculation and simulation on structural and electronic properties of metal-mediated base pair [39, 40]. Muller and Ono reported solution structure and crystal structure of DNA double helix with metal-mediated base pairs by NMR spectroscopy and X-ray respectively [41–43]. Some groups has also reported the conformational transition of oligonucleotides from random-coil single strand to hairpin-like con-

\* Author to whom correspondence should be addressed. E-mail: hjliang@ustc.edu.cn, FAX: +86-551-63607824, Tel.: +86-551-63607824

formation [24, 44]. However, the kinetics and mechanisms of such process, which contained the possible pathway of oligonucleotides folding as well as the folding intermediates and final state, were rarely investigated. Moreover, the behavior of oligonucleotides induced by different ions was also rarely studied.

To further understand the characteristic of the interaction between metal ions and oligonucleotides, isothermal titration calorimetry (ITC), circular dichroism (CD), and fluorescence spectroscopy were utilized to explore the behavior of oligonucleotides with  $\text{Hg}^{2+}$  and  $\text{Ag}^+$  and the differences of oligonucleotides behavior by changing the adding order of such two ions in this work. We design a special sequence of T-C-rich oligonucleotide (TCO) (5'-TTTTTT CCCCC TTTTT CCCCC TTTTT CCCCC TTTTT-3') which contains two kinds of repetitive functional segments, *i.e.*, six consecutive thymine bases and cytosine bases separated from each other. The sequence contains only C and T bases to avoid secondary structure and nonspecific binding. As expected, the oligonucleotides immediately started to form a relatively stable hairpin structure through the formation of T- $\text{Hg}^{2+}$ -T pairs upon the increase of  $\text{Hg}^{2+}$  concentration, and was further stabilized by the formation of C- $\text{Ag}^+$ -C pairs. However, the experimental result was amazing when the feeding sequence was changed. Unexpectedly, through careful speculation, it is found that TCO would also form a stable hairpin through the formation of an unconventional metal-base pair T- $\text{Ag}^+$ -C when  $\text{Ag}^+$  was first added. We have expanded research to discover the behavior of oligonucleotides induced by  $\text{Hg}^{2+}$  and  $\text{Ag}^+$  as well as the differences of hairpin-like structure and reaction pathway of T-C-rich oligonucleotides folding induced by varying the addition order of  $\text{Hg}^{2+}$  and  $\text{Ag}^+$ .

## II. EXPERIMENTS

### A. Chemicals and reagent

The oligonucleotide TCO and labeled TCO (TET-5'-TTTTTT CCCCC TTTTT CCCCC TTTTT CCCCC TTTTT-3'-BHQ-1) were synthesized and purified by HPLC from Shanghai Sangon Biotechnology Co., Ltd. (Shanghai, China). The labeled TCO was modified at the 5'-end with a tetrachloride fluorescein (TET) dye and at the 3'-end with a black hole quencher-1 (BHQ-1). Tris(hydroxymethyl)aminomethane (Tris), sodium acetate anhydrous (NaOAc), magnesium acetate tetrahydrate ( $\text{Mg}(\text{OAc})_2$ ), potassium nitrate ( $\text{KNO}_3$ ), and silver nitrate ( $\text{AgNO}_3$ ) were purchased from Sinopharm Chemical Reagent Co., Ltd. (Shanghai, China). Mercury(II) nitrate ( $\text{Hg}(\text{NO}_3)_2$ ) was obtained from Wanshan Mineral Products Company (Tongren, Guizhou, China). All salts were of analytical grade and used without further purification. The oligomer samples were

dissolved in buffer A consisting of 50 mmol/L Tris-HOAc, 100 mmol/L NaOAc, 0.005 mol/L  $\text{Mg}(\text{OAc})_2$ , and 0.03 mol/L  $\text{KNO}_3$  at pH=7.4. The oligomer solutions were then heated in a dry bath at 95 °C (ABSON, USA), equilibrated for 15 min at this temperature, and slowly cooled to room temperature. The concentration of oligonucleotide was measured by a UV-Vis spectrophotometer.

### B. Isothermal titration calorimetry

The most widely available isothermal titration calorimetry (ITC) used for micro-calorimetry of biological samples are based on the power-compensation principle. The temperature of each cell is monitored and maintained at a constant temperature through an electronic feedback loop that controls thermoelectric heaters located adjacent to each cell. When the titrant is added into the sample cell, the feedback loop will respond accordingly and record the heat change whether the reaction is exothermic or endothermic. Our ITC experiments were performed on a Microcal ITC200 (GE Healthcare) with the sample cell (0.199 mL) containing 10  $\mu\text{mol/L}$  oligonucleotide. The first experiment involved two steps, the  $\text{Hg}^{2+}$  step followed by the  $\text{Ag}^+$  step. Typically, the  $\text{Hg}(\text{NO}_3)_2$  solution was serially injected at 120 s intervals with continuous stirring of the solution at 1000 r/min in the sample cell till equilibrium. Then,  $\text{AgNO}_3$  solution was added into the sample cell. Raw calorimetric data were corrected for the heat of dilution of  $\text{Hg}^{2+}$  and oligonucleotide by subtracting the heat from the corresponding blank titrations. The comparison experiment was in reverse order, the  $\text{Ag}^+$  step followed by the  $\text{Hg}^{2+}$  step. Other condition and procedure were the same. Data analysis was performed using the MicroCal ORIGIN software.

### C. Circular dichroism

Circular dichroism (CD) spectra were measured using a JASCO J-810 spectropolarimeter at 25 °C. The oligomer concentration used was 10  $\mu\text{mol/L}$ . Each kind of metal ion was serially injected till equilibrium before another kind of metal was added. Each measurement was recorded from 235 nm to 330 nm at a scan rate of 100 nm/min using a sealed 1 mm path-length quartz cuvette. The spectra were collected with a response time of 0.1 s and data intervals of 0.2 nm. The final spectra were the averages of two measurements. The scan of the buffer alone under the same conditions was used as the blank, and was subtracted from the average scan for each sample.

### D. Fluorescence measurements

Fluorescence spectra were performed on a fluorolog-3 spectrofluorophotometer (Jobin Yvon SAS, France).

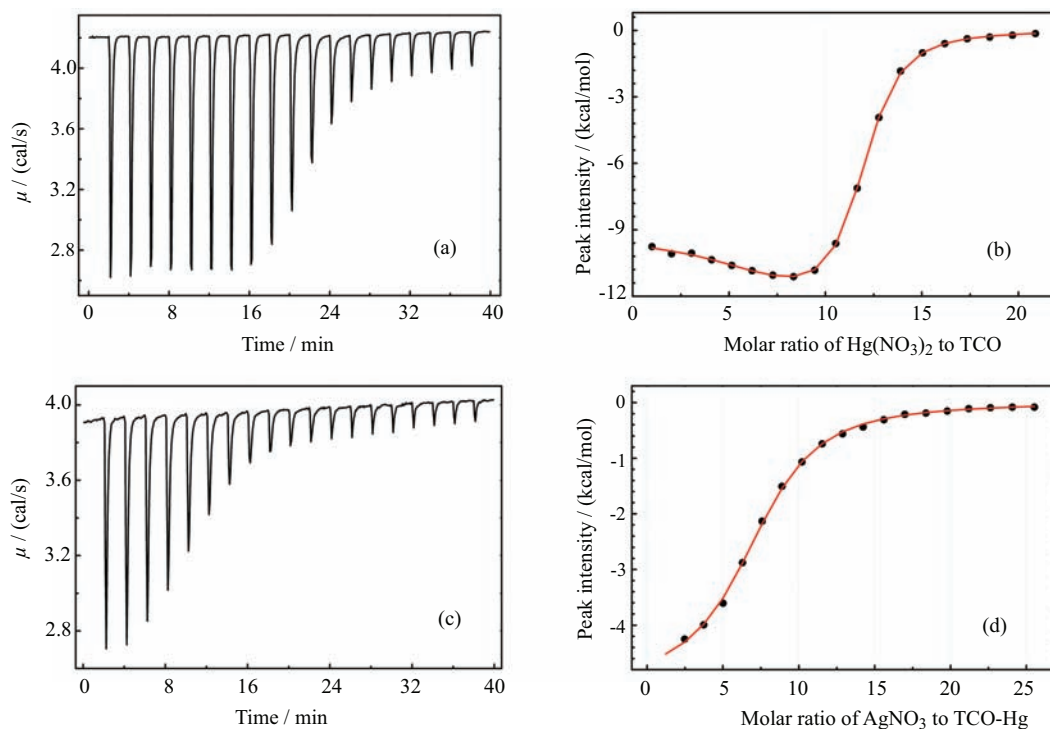


FIG. 1 Thermodynamic analyses of the interaction of  $\text{Hg}^{2+}$  and  $\text{Ag}^+$  with the oligonucleotide TCO (10  $\mu\text{mol/L}$ ). (a) Typical ITC profile of the interaction between  $\text{Hg}(\text{NO}_3)_2$  and TCO at 25 °C and pH=7.4 in buffer A. The curve shows the heat rate during the titration. (b) Thermogram of the integrated peak intensities plotted against the molar ratio of  $\text{Hg}(\text{NO}_3)_2$  to TCO. The fit shown as a solid line is for the “two sets of site model”. (c) Typical ITC profile of the interaction between  $\text{AgNO}_3$  and TCO-Hg complex. (d) Thermogram of the integrated peak intensities plotted against the molar ratio of  $\text{AgNO}_3$  to TCO-Hg complex. The fit shown as a solid line is for the “one sets of site model”.

Both the excitation and emission slit widths were set at 2.0 nm. TET was excited  $\lambda_{\text{ex}}=522$  nm, and its fluorescence emission was followed at  $\lambda_{\text{em}}=539$  nm. The initial oligomer concentrations were 200 nmol/L. After each 1  $\mu\text{L}$  addition of 80  $\mu\text{mol/L}$   $\text{Hg}(\text{NO}_3)_2$  or  $\text{AgNO}_3$  in comparison experiment, the fluorescence was measured with excitation at 522 nm.

### III. RESULTS AND DISCUSSION

#### A. Isothermal titration calorimetry

Kinetic and thermodynamic information can be obtained from ITC which is a powerful and versatile method to study the physical basis of molecular interactions. To explore the folding process of TCO induced by two metal ions, the thermodynamic properties of the interaction between TCO and two metal ions in buffer A at 25 °C and pH=7.4 were examined by ITC.

The ITC profiles of the sequential titration of  $\text{Hg}(\text{NO}_3)_2$  and  $\text{AgNO}_3$  to TCO are shown in Fig.1. As shown in Fig.1(a), each injection of  $\text{Hg}(\text{NO}_3)_2$  into TCO produced a sharp negative peak indicating an exothermic interaction. The released heat kept steady at a large level with the first eight injections and then decreased

until the reaction reached equilibrium. Figure 1(b) shows the integrated heats of binding obtained from the heat rate normalized to the moles of  $\text{Hg}^{2+}$  titrated, prior to subtracting the blank by injecting  $\text{Hg}(\text{NO}_3)_2$  into the same buffer. The value of ordinate began to decrease and then increased till equilibrium, which indicated the binding reaction had two different steps. Thus, the titration plot was a sigmoid curve using the “two sets of site model” (ITC data analysis in origin) fitting.

Table I summarizes the thermodynamic parameters of TCO binding  $\text{Hg}^{2+}$  and  $\text{Ag}^+$  successively which were obtained from Fig.1(b). The stoichiometry  $n$ , binding constant  $K$ , enthalpy change  $\Delta H$  and entropy change  $\Delta S$  for the specific binding between  $\text{Hg}^{2+}$  and TCO were obtained from the fitted curve, which were very helpful to understand and analyze the process of the titration reaction.

T-Hg-T structure is the most familiar and stable metal-base pair for  $\text{Hg}^{2+}$ . We suppose that the TCO prefers to adopt hairpin structure which will be explained later. Four T6 segments in TCO can form two sets of T6-(Hg)6-T6, that is,  $\text{Hg}^{2+}$  can interact with TCO at two different locations which agrees with the ITC fitting model. According to previous research [45, 46], it is supposed that TCO initially generated two

TABLE I ITC-derived thermodynamic parameters for the TCO oligonucleotide construct binding  $\text{Hg}^{2+}$  in and TCO-Hg complex binding  $\text{Ag}^+$  in buffer A. The units are as follows:  $K_1$  in  $10^6$  L/mol,  $K_2$  in  $10^5$  L/mol,  $\Delta H_1$  and  $\Delta H_2$  in kcal/mol,  $\Delta S_1$  and  $\Delta S_2$  in  $\text{mol}^{-1}\text{K}^{-1}$ .

	$n_1$	$K_1$	$\Delta H_1$	$\Delta S_1$	$n_2$	$K_2$	$\Delta H_2$	$\Delta S_2$
TCO-Hg	6.02±0.60	4.37±1.94	-9.24±0.29	-0.617	5.50±0.66	7.47±0.62	-13.35±0.86	-17.9
TCO-Hg-Ag					7.10±0.06	1.58±0.08	-5.05±0.07	6.85

kinds of intermediates induced by  $\text{Hg}^{2+}$ , in which  $\text{Hg}^{2+}$  preferentially bound closely to one end of hairpin loop and the opposite end of such loop, respectively. These two different pathways finally generated identical final product. The sum of binding number  $n_1$  and  $n_2$  for  $\text{Hg}^{2+}$  was 12, indicating the  $\text{Hg}^{2+}$  bound with the T:T mispair at a molar ratio of 1:1. Entropy represented the degree of freedom [47]. Therefore, the two negative  $\Delta S$  of two pathways indicated the processes with reduced entropy, which indicated a more ordered structure, *i.e.*, TCO changed from random coil to regular, stable hairpin when  $\text{Hg}^{2+}$  were added. The lower  $\Delta S_1$  showed that pathway 1 only was required to overcome small change of conformational entropy, indicating that the binding-site of  $\text{Hg}^{2+}$  was close to one end of the hairpin loop. Conversely, the binding-site of pathway 2 located at the opposite end of hairpin loop, in which remarkable conformational transition from a random coil to a hairpin occurred.

After the binding of  $\text{Hg}^{2+}$  reached equilibrium, further reaction with  $\text{Ag}^+$  addition was studied. Figure 1(c) shows a ITC profile of the interaction between  $\text{AgNO}_3$  and TCO-Hg complex, indicating that  $\text{Ag}^+$  could further enhance and stabilize the TCO-Hg complex through the formation of C-Ag-C structure. Figure 1(d) shows the thermogram of the integrated peak intensities plotted against the molar ratio of  $\text{AgNO}_3$  to TCO-Hg complex. The value of ordinate simply increased till equilibrium, which indicated that  $\text{Ag}^+$  could bind to such complex by only one pathway. The titration plot was fitted by using the “one set of site model”. As revealed in Table I, the binding number of  $\text{Ag}^+$  was 7 which indicated that six consecutive C:C mispairs in the middle of T6 segment and another loop base pair adjacent to the T-Hg-T pair took part in the binding. The Gibbs free energy change,  $\Delta G = \Delta H - T\Delta S$ . Thus, the observed negative  $\Delta H$  and positive  $\Delta S$  were favorable for the specific binding between  $\text{Ag}^+$  and C:C mismatched base pairs. If TCO began to form a duplex with  $\text{Hg}^{2+}$  addition, the average binding number for  $\text{Ag}^+$  of each TCO would be 9 because of no loop in duplex. Therefore, this result indicated that TCO finally adopted regular hairpin formation rather than duplex.

If we changed the feeding order of metal ions, *i.e.*  $\text{Hg}^{2+}$  followed by  $\text{Ag}^+$ , whether the result would still be the same as we expected that the two symmetric cytosine bases chain segment of TCO initially folded into metastable hairpin by  $\text{Ag}^+$ , and then  $\text{Hg}^{2+}$  per-

fecting the hairpin. However the experiment result was unexpected as below. The ITC profiles of the sequential titration of  $\text{AgNO}_3$  and  $\text{Hg}(\text{NO}_3)_2$  to TCO are shown in Fig.2. As shown in Fig.2(a), each injection of  $\text{AgNO}_3$  into TCO complex produced a sharper negative peak indicating an exothermic interaction. The heat released increased slowly with the five injections and then gradually decreased, the binding reaction did not reach equilibrium under the same experiment condition as we set previously. This phenomenon was different from Fig.1(c), indicating that no C-Ag-C generated. Figure 2(b) shows the integrated heats of binding obtained from the heat rate normalized to the moles of  $\text{Hg}^{2+}$  titrated. The value of ordinate also decreased first and then increased till equilibrium, which indicated the binding reaction also had two different steps. Thus, the titration plot was a sigmoid curve using the “two sets of site model” fitting.

Table II summarizes the thermodynamic parameters for TCO binding  $\text{Ag}^+$  and  $\text{Hg}^{2+}$  successively. The sum of binding number  $n_1$  and  $n_2$  for  $\text{Ag}^+$  was 16 which was much larger than the total number of C:C mispairs which is generally supposed to specifically capture  $\text{Ag}^+$ , indicating that not only cytosine bases but also other bases participated in the binding reaction of  $\text{Ag}^+$ . The two  $\Delta S$  with distinct difference showed that there were also two different pathways for  $\text{Ag}^+$  binding which was similar to  $\text{Hg}^{2+}$ . But the rate constant of  $\text{Ag}^+$  binding was lower than that of  $\text{Hg}^{2+}$  which signified that the T-Hg-T structure was more stable. Moreover, the much higher  $\Delta S_1$  and larger  $n_1$  may indicate that pathway 1 dominated the TCO folding. The positive  $\Delta S_2$  value may be attributed to the  $\text{Ag}^+$  dehydration according to recent research [43, 48]. Figure 2(c) shows a ITC profile of the interaction between  $\text{Hg}(\text{NO}_3)_2$  and TCO-Ag complex. The interaction between TCO-Ag complex and  $\text{Hg}^{2+}$  was very weak and reached terminal soon. The negative  $\Delta S$  in Table II also indicated a more ordered structure (hairpin or duplex). The binding number of  $\text{Hg}^{2+}$  is only 3 which is much smaller than previous result, suggesting only six T bases remained for  $\text{Hg}^{2+}$  binding in TCO-Ag complex. It thus triggers us to think where the left T bases are. Moreover, T:T mispair cannot bind  $\text{Ag}^+$  as we investigated and reported [49]. Based on the above discussion, it can only be surmised that many T bases were involved in the binding of  $\text{Ag}^+$ , *i.e.*, an unusual metal-base pair containing T base for  $\text{Ag}^+$  was obtained.

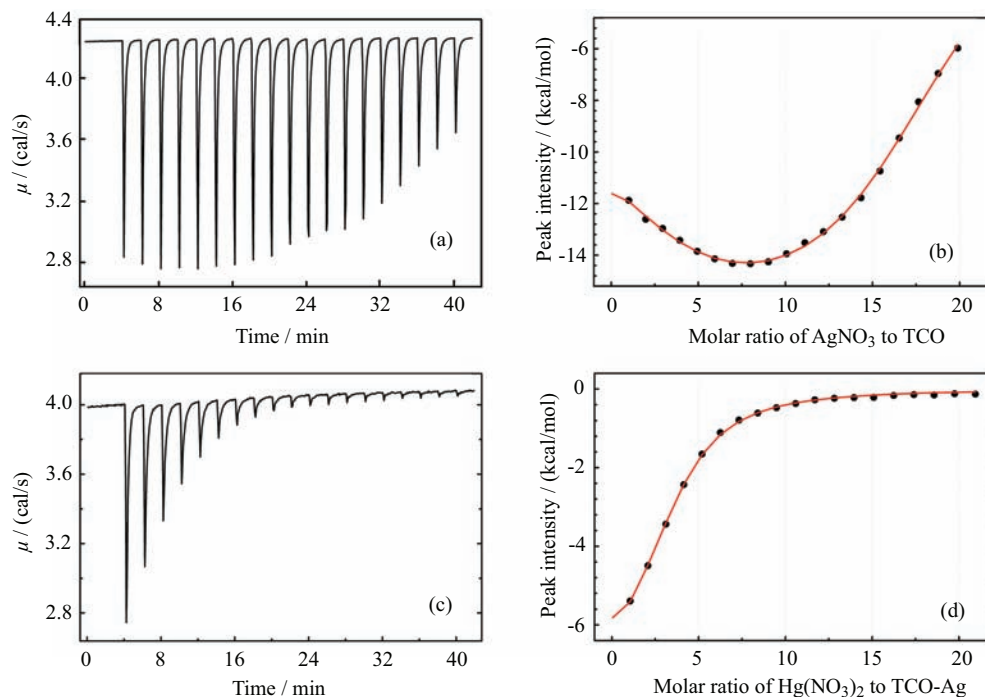


FIG. 2 Thermodynamic analyses of the interaction of  $\text{Ag}^+$  and  $\text{Hg}^{2+}$  with the oligonucleotide TCO (10  $\mu\text{mol/L}$ ). (a) Typical ITC profile of the interaction between  $\text{AgNO}_3$  and TCO at 25  $^\circ\text{C}$  and  $\text{pH}=7.4$  in buffer A. The curve shows the heat rate during the titration. (b) Thermogram of the integrated peak intensities plotted against the molar ratio of  $\text{AgNO}_3$  to TCO. The fit shown as a solid line is for the “two sets of site model”. (c) Typical ITC profile of the interaction between  $\text{Hg}(\text{NO}_3)_2$  and TCO-Ag complex. (d) Thermogram of the integrated peak intensities plotted against the molar ratio of  $\text{Hg}(\text{NO}_3)_2$  to TCO-Ag complex. The solid line is for the fitting result of the “one sets of site model”.

TABLE II ITC-derived thermodynamic parameters for the TCO oligonucleotide construct binding  $\text{Ag}^+$  ions and TCO-Ag complex binding  $\text{Hg}^{2+}$  in buffer A. The units are as follows:  $K_1$  in  $10^6$  L/mol,  $K_2$  in  $10^5$  L/mol,  $\Delta H_1$  and  $\Delta H_2$  in kcal/mol,  $\Delta S_1$  and  $\Delta S_2$  in  $\text{mol}^{-1}\text{K}^{-1}$ .

	$n_1$	$K_1$	$\Delta H_1$	$\Delta S_1$	$n_2$	$K_2$	$\Delta H_2$	$\Delta S_2$
TCO-Ag	$14.12 \pm 0.54$	$1.26 \pm 0.15$	$17.57 \pm 1.03$	-35.6	$2.47 \pm 0.39$	$7.54 \pm 4.72$	$-7.69 \pm 3.63$	1.09
TCO-Ag-Hg					$3.26 \pm 0.05$	$1.00 \pm 0.04$	$-7.62 \pm 0.14$	-2.69

## B. Circular dichroism

CD is a general technique to sensitively monitor the conformation transition of anisotropic molecules and chiral super assemblies, has been used extensively in the study of nucleic acids especially secondary structures such as hairpin, G-quadruplex and so on. To further study TCO binding characteristic with metal ions, CD was performed to analyse the change of secondary structure. The “TCO-Hg- $n_1$ ” and “TCO-Hg-Ag- $n_2$ ” represented  $n_1$  injections of  $\text{Hg}^{2+}$  into TCO, and  $n_2$  injections of  $\text{Ag}^+$  into TCO-Hg complex, other descriptions were similar as in Fig.3. As revealed in Fig.3(a), the positive peak at 280 nm reduced rapidly and the negative peak at 270 nm started to appear with the first addition of  $\text{Hg}^{2+}$ , interpreting the gradual transition of TCO from random coiled single chain to ordered hairpin structure. Along with the increase of  $\text{Hg}^{2+}$ , the change decreased until two adjacent curves

were nearly overlapped, signified the equilibrium of the binding reaction with  $\text{Hg}^{2+}$ . Thus, a relatively stable hairpin structure was formed by  $\text{Hg}^{2+}$ . The system was activated by  $\text{Ag}^+$  after the end point of reaction with  $\text{Hg}^{2+}$ . The negative peak represented hairpin structure increased sharply till equilibrium, indicating that the TCO-Hg complex formed a more ordered and perfect hairpin configuration by  $\text{Ag}^+$ . Next we changed the order of such two ions addition. As shown in Fig.3(b), the peak of single chain disappeared more rapidly and the peak of hairpin arose meanwhile along with the addition of  $\text{Ag}^+$ , which revealed that TCO formed hairpin structure more easily by  $\text{Ag}^+$ . The conformational change stopped till large amount of  $\text{Ag}^+$  addition which is in accordance with big binding-site number from ITC data. It appeared that there was no significant conformational change of TCO-Ag complex by  $\text{Hg}^{2+}$  which indicated that  $\text{Hg}^{2+}$  was not in the form of hairpin. Besides, it was observed that the depth and the posi-

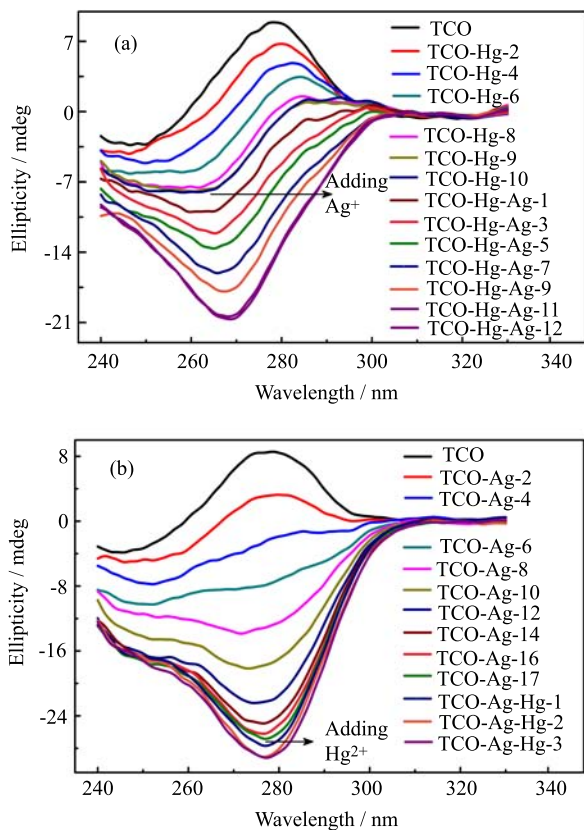


FIG. 3 CD spectral change of TCO (10  $\mu\text{mol/L}$ ) in the presence of increasing  $\text{Hg}(\text{NO}_3)_2$  and  $\text{AgNO}_3$  concentrations at 25  $^\circ\text{C}$  and  $\text{pH}=7.4$  in buffer A. (a)  $\text{AgNO}_3$  followed by  $\text{Hg}(\text{NO}_3)_2$ . (b)  $\text{Hg}(\text{NO}_3)_2$  followed by  $\text{AgNO}_3$ .

tion of the peak represented different hairpin structures. In conclusion, CD data revealed that the folding process of TCO driven by metal ions was different by the modulation of metal ions addition sequence.

### C. Fluorescence measurements

The folding processes of TCO driven by  $\text{Hg}^{2+}$  and  $\text{Ag}^+$  respectively were also monitored and analyzed by fluorescence spectra. Double-labeled TCO (DL-TCO) was modified by tetrachloride fluorescein (TET) at 5'-terminal and black hold quencher-1 (BHQ-1) at 3'-terminal of TCO. The fluorescence intensity will be strong when TET separated from BHQ-1, otherwise it is weak. Therefore, the variation of fluorescence intensity was indirectly utilized to reflect the formation of hairpin structure. As shown in Fig.4, the emission intensity was extremely strong when DL-TCO existed solely without any ions, indicating that DL-TCO was in form of random-coil single chain. Whether  $\text{Hg}^{2+}$  or  $\text{Ag}^+$  were added, the fluorescence intensity reduced significantly with increase of ions concentration, revealing that both ends of DL-TCO were gradually close to each other, *i.e.*, DL-TCO was folded into hairpin structure

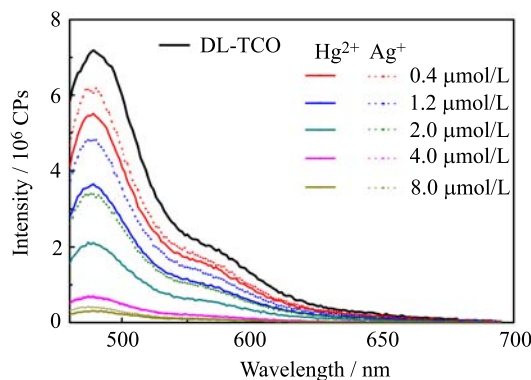


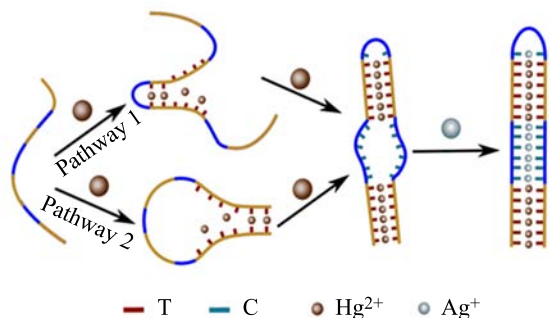
FIG. 4 Fluorescence spectra of DL-TCO folding driven by  $\text{Hg}^{2+}$  and  $\text{Ag}^+$  respectively. The black solid line represented DL-TCO without any ions. The solid lines and the dotted lines represented adding  $\text{Hg}^{2+}$  and  $\text{Ag}^+$  to DL-TCO, respectively.

with either ions. Moreover, the fluorescence intensity of  $\text{Ag}^+$  was much higher than that of  $\text{Hg}^{2+}$  at low concentration, suggesting that the TCO folding was dominated by pathway 1 with  $\text{Ag}^+$  intercalation, and was a little higher at high concentration, indicating that TCO formed similar stable hairpin structure induced by two ions and both ends of DL-TCO-Ag complex slightly separated from each other. The fluorescence spectral verified that hairpin structure formed with the addition of ions and the two final hairpin structures induced by altering the adding order of two ions were different, which was in agreement with CD data.

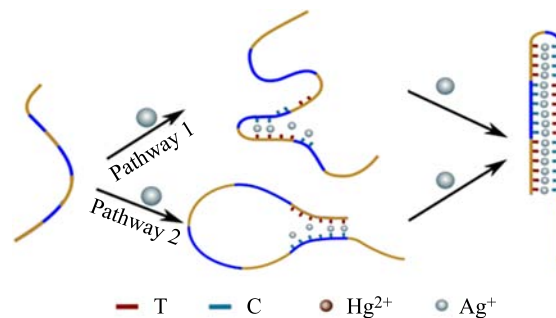
### D. The mechanism of TCO oligonucleotide folding driven by $\text{Hg}^{2+}$ and $\text{Ag}^+$

Through three characterization methods as described above: ITC, CD, and fluorescence spectrum, thorough study of TCO oligonucleotide folding mechanisms driven by two ions was performed. The differences between two ions feeding sequences were discussed individually. First, for the condition of the addition of  $\text{Ag}^+$  followed by  $\text{Hg}^{2+}$  to TCO, all the T bases of TCO firstly formed T-Hg-T structure by  $\text{Hg}^{2+}$  to generate a hairpin configuration through two different pathways (Scheme 1). It is supposed that TCO initially produced two kinds of intermediates induced by  $\text{Hg}^{2+}$ , in which  $\text{Hg}^{2+}$  preferentially bound closely to the end of hairpin loop and the opposite end of such loop, respectively. These two different pathways finally generated identical final product. After the binding with  $\text{Hg}^{2+}$  reached equilibrium, the remaining C bases except the ones in the four-membered loop of hairpin formed C-Ag-C structure by  $\text{Ag}^+$  to produce a more stabilized and perfect hairpin through only one pathway. The mechanism as proposed in Scheme 1 is in good agreement with all experimental data.





Scheme 1 Binding directions of  $\text{Hg}^{2+}$  and  $\text{Ag}^+$  to the TCO oligonucleotides. The blue lines represent the spacing sequences of cytosine bases, whereas the orange lines indicate the sequences of thymine bases.



Scheme 2 Binding directions of  $\text{Ag}^+$  and  $\text{Hg}^{2+}$  to the TCO oligonucleotides. The blue lines represent the spacing sequences of cytosine bases, whereas the orange lines indicate the sequences of thymine bases.

Next more attention was paid to speculating the mechanism of TCO folding driven by  $\text{Ag}^+$  and  $\text{Hg}^{2+}$  successively. The TCO oligonucleotide can only form three kinds of base pair as follows: C-C, T-T, and T-C due to the existence of only two kinds of bases. The binding-site number 16 for  $\text{Ag}^+$  was much larger than the maximum number 9 of possible C-C base pairs which were generally supposed to specifically bind  $\text{Ag}^+$ . Moreover, further addition of  $\text{Hg}^{2+}$  has little effect on hairpin and only three binding-sites for  $\text{Hg}^{2+}$ , representing that the remaining six T bases may exist at one side of TCO in the form of six consecutive thymine chain segment rather than further form more stable hairpin. Then other thymine bases have two purposes at the most that one part possibly constitute the loop of hairpin and another may take part in the formation of metal-base pair (T-T or T-C) for  $\text{Ag}^+$ . However, T-T mispair cannot bind  $\text{Ag}^+$  according to our previous research [49]. Then,  $\text{Ag}^+$  can only exist in two structures: C- $\text{Ag}^+$ -C and T- $\text{Ag}^+$ -C. Hairpin with four-membered loop was relatively stable because of the combined impact of the ring tension and metal-base pair force. We supposed that four T bases formed the loop. There were six T bases for  $\text{Hg}^{2+}$  binding. Therefore, at least 14 T bases formed a new metal-base pair: T- $\text{Ag}^+$ -C. The number of C- $\text{Ag}^+$ -C structure was at most two. No matter there was one or two C- $\text{Ag}^+$ -C, the TCO was unable to form a stable hairpin. Thus, we inferred that during the first addition of  $\text{Ag}^+$  into the TCO, no C- $\text{Ag}^+$ -C existed, that is, the new metal-base pair T- $\text{Ag}^+$ -C was the only form for  $\text{Ag}^+$  binding. This metal-base pair T- $\text{Ag}^+$ -C, which has been reported by Hidehito Urata and Ono, has roughly comparable thermal stability to the C- $\text{Ag}^+$ -C base pair [20, 21, 50], indicating that the free energy of generating one T- $\text{Ag}^+$ -C structure is roughly equivalent to that of generating one C- $\text{Ag}^+$ -C structure. Moreover, beginning to generate the C- $\text{Ag}^+$ -C structure needed to overcome more conformational entropy change. Besides the number of T-C base pair is much larger than that of C-C base pair, the TCO oligonucleotide will prefer to form more stable structure in free energy including

T- $\text{Ag}^+$ -C base pair when first adding  $\text{Ag}^+$ . In addition, those sixteen T- $\text{Ag}^+$ -C metal-base pair should be consecutive without mispair in hairpin because the TCO- $\text{Ag}^+$  hairpin is also stable enough and is unable to be further stabilized by  $\text{Hg}^{2+}$ . Among all twenty-four T bases, sixteen forming T- $\text{Ag}^+$ -C base pairs and six for further interaction with  $\text{Hg}^{2+}$ , there are two remaining T bases constituting the loop of hairpin with two remaining C bases.

In conclusion, it is inferred that the mechanism of TCO folding is driven by  $\text{Ag}^+$  and  $\text{Hg}^{2+}$  successively, as shown in Scheme 2. The formation of T- $\text{Ag}^+$ -C structure consumed large amount of T bases, sharply reducing the binding ability with  $\text{Hg}^{2+}$  subsequently. Based on ITC and CD data, it is proposed that TCO- $\text{Ag}^+$  complex can dimerize through the overhang T6 chain segment crosslinked by  $\text{Hg}^{2+}$ . The dimerization which have little effect on hairpin structure provides six binding-site, so the average binding-site number  $n_2$  for  $\text{Hg}^{2+}$  is three for each TCO- $\text{Ag}^+$  molecule. Both ends of TCO- $\text{Ag}^+$  complex slightly separate from each other, thereby, presenting a higher fluorescence intensity when DL-TCO binding with  $\text{Ag}^+$  than that of  $\text{Hg}^{2+}$  at the same concentration. Therefore, the proposed mechanism of TCO folding driven by  $\text{Ag}^+$  and  $\text{Hg}^{2+}$  successively is also in very good agreement with all experiment data. At last, we turned back to the explanation of the mechanism of TCO folding by  $\text{Hg}^{2+}$  and  $\text{Ag}^+$  successively. Why didn't the TCO form T- $\text{Hg}^{2+}$ -C structure with first adding  $\text{Hg}^{2+}$ ? According to the investigation by Ono group, T- $\text{Hg}^{2+}$ -T was more thermally stable than T- $\text{Hg}^{2+}$ -C [20]. If the TCO was folded similarly as Scheme 2, TCO- $\text{Hg}^{2+}$  complex was unable to be further stabilized by  $\text{Ag}^+$  which did not agree with ITC and CD data. Therefore, it is verified that the mechanism proposed in Scheme 1 is correct.

#### IV. CONCLUSION

This study further extended our understanding of metal-DNA complex characteristics. Utilizing three

characterization methods of ITC, CD, and fluorescence spectrum, the mechanism and secondary structural change of TCO driven by metal ions were investigated. The differences of the mechanism and conformational change of TCO oligonucleotides driven by different orders of  $\text{Hg}^{2+}$  and  $\text{Ag}^+$  addition were mainly discussed. The mechanism of TCO driven by  $\text{Hg}^{2+}$  and  $\text{Ag}^+$  successively was that all the T bases of TCO firstly formed T-Hg-T structure by  $\text{Hg}^{2+}$  through two different pathways and then the remaining C bases except which in the four-membered loop of hairpin formed C-Ag-C structure by  $\text{Ag}^+$  through only one pathway. However, the mechanism and folding process were distinctly different by only varying the feeding order of two ions. A new experimental evidence of an unusual metal-base pair T-Ag-C was obtained by carefully deducing with first addition of  $\text{Ag}^+$ . Then the TCO-Ag complex was dimerized by  $\text{Hg}^{2+}$ . In summary, we discovered an interesting phenomenon that the behavior of oligonucleotide was remarkably different by just varying the order of metal ions addition. This work provides a promising strategy for the investigation of the mechanism and structural transformation of oligonucleotides influenced by different metal ions and different orders of metal ions addition, which can eventually lead to progress in constructing metal-triggered DNA machines, DNA molecular logic operation and metal-containing DNA nanotechnology. Moreover, previous metal-base pairs are mostly discovered by analyzing thermal stability of nucleic acids. Therefore, this study will provides a new strategy to explore and discover new metal-base pair.

## V. ACKNOWLEDGMENTS

This work was supported by the National Natural Science Foundation of China (No.20934004 and No.91127046), the National Basic Research Program of China (No.2012CB821500 and No.2010CB934500), the Foundation for Scholar of Hefei Normal University (No.2014rcjj03), and the Foundations of Educational Committee of Anhui Province (No.KJ2014A205).

- [1] F. A. Aldaye, A. L. Palmer, and H. F. Sleiman, *Science* **321**, 1795 (2008).
- [2] Z. Wang and Y. Lu, *J. Mater. Chem.* **19**, 1788 (2009).
- [3] N. C. Seeman, *Nature* **421**, 427 (2003).
- [4] J. J. Storhoff and C. A. Mirkin, *Chem. Rev.* **99**, 1849 (1999).
- [5] J. Muller, *Nature* **444**, 698 (2006).
- [6] K. Tanaka, G. H. Clever, Y. Takezawa, Y. Yamada, C. Kaul, M. Shionoya, and T. Carell, *Nat. Nanotechnol.* **1**, 190 (2006).
- [7] G. H. Clever, C. Kaul, and T. Carell, *Angew. Chem. Int. Ed.* **46**, 6226 (2007).
- [8] G. H. Clever and M. Shionoya, *Coord. Chem. Rev.* **254**, 2391 (2010).
- [9] J. Mueller, *Eur. J. Inorg. Chem.* 3749 (2008).
- [10] Y. Takezawa and M. Shionoya, *Acc. Chem. Res.* **45**, 2066 (2012).
- [11] N. A. Froystein and E. Sletten, *J. Am. Chem. Soc.* **116**, 3240 (1994).
- [12] A. Ono, S. Cao, H. Togashi, M. Tashiro, T. Fujimoto, T. Machinami, S. Oda, Y. Miyake, I. Okamoto, and Y. Tanaka, *Chem. Commun.* 4825 (2008).
- [13] E. Meggers, P. L. Holland, W. B. Tolman, F. E. Romesberg, and P. G. Schultz, *J. Am. Chem. Soc.* **122**, 10714 (2000).
- [14] C. Switzer, S. Sinha, P. H. Kim, and B. D. Heuberger, *Angew. Chem. Int. Ed.* **44**, 1529 (2005).
- [15] J. S. Lee, L. J. P. Latimer, and R. S. Reid, *Biochem. Cell Biol.* **71**, 162 (1993).
- [16] K. Tanaka, A. Tengeji, T. Kato, N. Toyama, M. Shiro, and M. Shionoya, *J. Am. Chem. Soc.* **124**, 12494 (2002).
- [17] G. H. Clever, K. Polborn, and T. Carell, *Angew. Chem. Int. Ed.* **44**, 7204 (2005).
- [18] Y. Miyake, H. Togashi, M. Tashiro, H. Yamaguchi, S. Oda, M. Kudo, Y. Tanaka, Y. Kondo, R. Sawa, T. Fujimoto, T. Machinami, and A. Ono, *J. Am. Chem. Soc.* **128**, 2172 (2006).
- [19] Y. Tanaka, S. Oda, H. Yamaguchi, Y. Kondo, C. Kojima, and A. Ono, *J. Am. Chem. Soc.* **129**, 244 (2007).
- [20] A. Ono, H. Torigoe, Y. Tanaka, and I. Okamoto, *Chem. Soc. Rev.* **40**, 5855 (2011).
- [21] H. Urata, E. Yamaguchi, Y. Nakamura, and S. Wada, *Chem. Commun.* **47**, 941 (2011).
- [22] T. Funai, Y. Miyazaki, M. Aotani, E. Yamaguchi, O. Nakagawa, S. Wada, H. Torigoe, A. Ono, and H. Urata, *Angew. Chem. Int. Ed.* **51**, 6464 (2012).
- [23] F. A. Polonius and J. Muller, *Angew. Chem. Int. Ed.* **46**, 5602 (2007).
- [24] A. Ono and H. Togashi, *Angew. Chem. Int. Ed.* **43**, 4300 (2004).
- [25] J. S. Lee, M. S. Han, and C. A. Mirkin, *Angew. Chem. Int. Ed.* **46**, 4093 (2007).
- [26] Z. Lin, X. Li, and H. B. Kraatz, *Anal. Chem.* **83**, 6896 (2011).
- [27] C. W. Liu, C. C. Huang, and H. T. Chang, *Anal. Chem.* **81**, 2383 (2009).
- [28] C. Y. Lin, C. J. Yu, Y. H. Lin, and W. L. Tseng, *Anal. Chem.* **82**, 6830 (2010).
- [29] N. Graf, M. Goritz, and R. Kramer, *Angew. Chem. Int. Ed.* **45**, 4013 (2006).
- [30] D. Li, A. Wieckowska, and I. Willner, *Angew. Chem. Int. Ed.* **47**, 3927 (2008).
- [31] Z. G. Wang, J. Elbaz, and I. Willner, *Nano Lett.* **11**, 304 (2011).
- [32] A. Porchetta, A. Vallee-Belisle, K. W. Plaxco, and F. Ricci, *J. Am. Chem. Soc.* **135**, 13238 (2013).
- [33] S. Bi, B. Ji, Z. P. Zhang, and J. J. Zhu, *Chem. Sci.* **4**, 1858 (2013).
- [34] R. Freeman, T. Finder, and I. Willner, *Angew. Chem. Int. Ed.* **48**, 7818 (2009).
- [35] K. S. Park, C. Jung, and H. G. Park, *Angew. Chem. Int. Ed.* **49**, 9757 (2010).
- [36] G. Y. Zhang, W. L. Lin, W. Q. Yang, Z. Y. Lin, L. H. Guo, B. Qiu, and G. N. Chen, *Analyst* **137**, 2687 (2012).



- [37] H. Torigoe, Y. Miyakawa, A. Ono, and T. Kozasa, *Nucleosides Nucleotides Nucleic Acids* **30**, 149 (2011).
- [38] H. Torigoe, Y. Miyakawa, A. Ono, and T. Kozasa, *Thermochim. Acta* **532**, 28 (2012).
- [39] M. Fuentes-Cabrera, B. G. Sumpter, J. E. Sponer, J. Sponer, L. Petit, and J. C. Wells, *J. Phys. Chem. B* **111**, 870 (2007).
- [40] H. Miyachi, T. Matsui, Y. Shigeta, and K. Hirao, *PCCP* **12**, 909 (2010).
- [41] S. Johannsen, N. Megger, D. Bohme, R. K. O. Sigel, and J. Muller, *Nat. Chem.* **2**, 229 (2010).
- [42] J. Kondo, T. Yamada, C. Hirose, I. Okamoto, Y. Tanaka, and A. Ono, *Angew. Chem. Int. Ed.* **53**, 2385 (2014).
- [43] H. Yamaguchi, J. Sebera, J. Kondo, S. Oda, T. Komuro, T. Kawamura, T. Dairaku, Y. Kondo, I. Okamoto, A. Ono, J. V. Burda, C. Kojima, V. Sychrovsky, and Y. Tanaka, *Nucleic Acids Res.* **42**, 4094 (2014).
- [44] Y. Wang, Y. Zheng, F. Yang, and X. R. Yang, *Chem. Commun.* **48**, 2873 (2012).
- [45] G. R. Bowman, X. Huang, Y. Yao, J. Sun, G. Carlsson, L. J. Guibas, and V. S. Pande, *J. Am. Chem. Soc.* **130**, 9676 (2008).
- [46] E. J. Sorin, Y. M. Rhee, B. J. Nakatani, and V. S. Pande, *Biophys. J.* **85**, 790 (2003).
- [47] H. Torigoe, A. Ono, and T. Kozasa, *Chem-Eur. J.* **16**, 13218 (2010).
- [48] H. Torigoe, I. Okamoto, T. Dairaku, Y. Tanaka, A. Ono, and T. Kozasa, *Biochimie* **94**, 2431 (2012).
- [49] W. Ding, W. Deng, H. Zhu, and H. J. Liang, *Chem. Commun.* **49**, 9953 (2013).
- [50] T. Funai, J. Nakamura, Y. Miyazaki, R. Kiri, O. Nakagawa, S. Wada, A. Ono, and H. Urata, *Angew. Chem. Int. Edit.* **53**, 6624 (2014).